

have insufficient signal to noise to carry out a spectral interpretation. In this section we address two ways in which this difficulty is overcome in our work.

The first consideration is the instrument on which absorption spectra are obtained. In a normal scanning instrument, every wavelength point is subject to random noise generated during the time the spectrometer is tuned to that particular wavelength. The result is a low-intensity but high-frequency noise that may be convoluted on an absorption spectrum. Although this noise may not be an important problem in monitoring the pure absorption spectrum, as demonstrated above, peaks with smaller bandwidths are enhanced greatly in the higher order derivatives. Thus, noise and its associated small bandwidth will be greatly enhanced. Our spectra have been obtained with a diode array absorption spectrometer, however, and this high-frequency noise is eliminated since the spectrum is not collected from point to point. All wavelengths are collected simultaneously. The availability of these detection systems is the primary reason higher order derivatives of absorption spectra can be obtained.

The numerical methods chosen to find derivatives are also an important consideration in establishing the signal to noise. Derivatives were carried out using the techniques described by Butler and Hopkins.<sup>18</sup> These authors showed both experimentally and theoretically that the up to 4 times enhancement in the signal to noise of the derivative spectra could be obtained by careful consideration of the derivative intervals. Specifically for a linear array, the fourth derivative intervals should differ by 2, 1, 1, and 1 intervals. For example, in our spectra, which are digitized at 2-nm intervals, the first derivative is taken for differences every 10 nm (5 "intervals"), the second every 6 nm (3 "intervals"), the third every 4 nm (2 "intervals"), and the fourth every 2 nm (1 "interval"), leading to the 2, 1, 1, and 1 interval differences needed for the best signal to noise.

With the combination of the diode array absorption spectrometer and the Butler/Hopkins numerical method, derivatives could be obtained directly from the data. No data smoothing was found to be necessary, and more than sufficient signal to noise was obtained.

## Concerning the Crystal Structure of Porphine: A Proton Pulsed and <sup>13</sup>C CPMAS NMR Study

Lucio Frydman,<sup>†</sup> Alejandro C. Olivieri,<sup>†</sup> Luis E. Diaz,<sup>†</sup> Benjamin Frydman,<sup>\*,†</sup> Irina Kustanovich,<sup>‡</sup> and Shimon Vega<sup>‡</sup>

*Contribution from the Facultad de Farmacia y Bioquímica, Universidad de Buenos Aires, Junin 956, 1113 Buenos Aires, Argentina, and the Department of Isotope Research, The Weizmann Institute of Sciences, 76100 Rehovot, Israel. Received May 31, 1988*

**Abstract:** Solid-state NMR techniques were employed in order to study the structure and the dynamics of porphine. The changes observed in the line width of the <sup>1</sup>H NMR signal between 173 and 443 K suggest that the porphine macrocycles rotate in the crystals. This was confirmed by recording the <sup>13</sup>C CPMAS NMR spectra at different temperatures which showed, in addition to the expected coalescence of signals due to the central hydrogens tautomerism, a broadening of the resonances due to the overall molecular rotation. These studies, coupled to measurements at different temperatures and fields of the relaxation times of the <sup>1</sup>H magnetization in the rotating frame, allowed us to obtain activation parameters for the motion which are, within experimental error, equal to those made available by CPMAS NMR for the tautomerism of the central hydrogens. These results suggest an explanation for what seems to be a contradiction between the structure of porphine observed by X-ray, according to which the central hydrogens are localized in opposite pairs of nitrogens, and the structure observed by CPMAS in which the hydrogens migrate between the four central nitrogens. If it is assumed that the migration of the central hydrogens is coupled to a 90° rotation of the molecules, the translational symmetry of the crystal will not be changed by the tautomerism, and an X-ray analysis would always detect a single tautomer.

Free-base porphyrins possess two inner hydrogens bonded to opposite pairs of nitrogen atoms. Since there are four such atoms in porphyrins, the central hydrogens can jump between two different configurations (Figure 1) giving rise to a tautomeric process which has been extensively studied by <sup>1</sup>H, <sup>13</sup>C, and <sup>15</sup>N variable-temperature solution NMR both in symmetrically<sup>1-12</sup> as well as in asymmetrically<sup>13-15</sup> substituted porphyrins. These studies have shown that in the former molecules, the hydrogens migrate in an effective double minimum potential between two equally populated tautomers A and B with a rate which at room temperature is fast on the NMR time scale (ca. 10<sup>3</sup> Hz). The tautomeric behavior of these free-base porphyrins has also been recently explored in the solid state by means of <sup>13</sup>C and <sup>15</sup>N CPMAS NMR,<sup>16-20</sup> where it was found that the symmetry of the double minimum potential may be perturbed by the crystal packing forces. Nevertheless in at least two porphyrins, *meso*-tetra-

tolylporphyrin and porphine, the kinetic behavior of the central hydrogens in the solid state was found to be similar to the one

- (1) Storm, C. B.; Teklu, Y. *J. Am. Chem. Soc.* **1972**, *94*, 1745.
- (2) Abraham, R. J.; Hawkes, G.; Smith, K. *Tetrahedron Lett.* **1974**, 1483.
- (3) Eaton, S. S.; Eaton, G. R. *J. Am. Chem. Soc.* **1977**, *99*, 1601.
- (4) Gust, D.; Roberts, J. D. *J. Am. Chem. Soc.* **1977**, *99*, 3637.
- (5) Yeh, H. J. C.; Sato, M.; Morishima, I. *J. Magn. Reson.* **1977**, *26*, 365.
- (6) Limbach, H.-H.; Hennig, J. *J. Chem. Soc., Faraday Trans II* **1979**, *75*, 752.
- (7) Limbach, H.-H.; Hennig, J. *J. Chem. Phys.* **1979**, *71*, 3120.
- (8) Limbach, H.-H.; Hennig, J.; Gerritzen, D.; Rumpel, H. *Faraday Discuss. Chem. Soc.* **1982**, *74*, 229.
- (9) Limbach, H.-H.; Hennig, J.; Stulz, J. *J. Chem. Phys.* **1983**, *78*, 5432.
- (10) Hennig, J.; Limbach, H.-H. *J. Am. Chem. Soc.* **1984**, *106*, 292.
- (11) Stilbs, P.; Moseley, M. E. *J. Chem. Soc., Faraday Trans. II* **1980**, *76*, 729.
- (12) Stilbs, P. *J. Magn. Reson.* **1984**, *58*, 152.
- (13) Crossley, M. J.; Harding, M. M.; Sternhell, S. *J. Am. Chem. Soc.* **1986**, *108*, 3608.
- (14) Crossley, M. J.; Field, L. D.; Harding, M. M.; Sternhell, S. *J. Am. Chem. Soc.* **1987**, *109*, 2335.

<sup>†</sup> University of Buenos Aires.

<sup>‡</sup> The Weizmann Institute of Sciences.

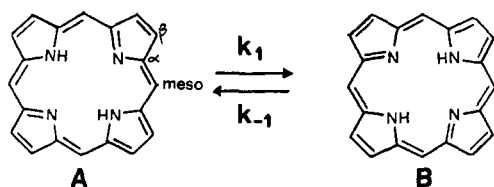


**Figure 1.** Scheme of the tautomerism of the central hydrogens of free-base porphine, showing the labeling of the atoms.

present in solution. For porphine (Figure 1), this similarity was rather unexpected since the X-ray study of this compound showed the hydrogens localized in opposite pairs of nitrogen.<sup>21</sup> Moreover, although it could be argued that X-ray diffraction is not the best method to locate a hydrogen atom bonded to an electronegative atom,<sup>22</sup> the X-ray analysis of porphine also suggested the presence of localized hydrogens since it revealed that the heavier atoms of the skeleton were distorted toward the  $D_{2h}$ -like configuration which should arise from static central hydrogens.

Since one of the potential advantages of solid-state studies is that the positions of the atoms can be accurately known from crystallographic measurements (a situation not usually found in solution studies), it should be possible to draw general mechanistic conclusions about dynamic processes if NMR and X-ray results could be reconciled. Indeed, many cases have been reported in which solid-state NMR detects the presence of a motion in what X-ray presents as a motionless crystalline solid.<sup>23</sup> These potential contradictions, which are usually observed in molecules which possess aromatic or tetrahedron-like groups, can be solved by noting that if the jump of the molecule or of a particular group coincides with one of its symmetry operations, no disorder will be introduced in the crystal lattice. This could also be the case for porphine, whose highly planar and symmetric molecules may be performing 90° in-plane jumps in the solid. It is the purpose of the present study to explore, with the aid of  $^1\text{H}$  wide line and  $^{13}\text{C}$  CPMAS NMR techniques, this possibility.

The second moment ( $M_2$ ) of the  $^1\text{H}$  signal was measured between 173 and 443 K and showed a decrease which suggests the presence of an overall molecular motion. The relaxation times  $T_{1\rho}$  of the  $^1\text{H}$  magnetization were measured at different temperatures and allowed to obtain the activation parameters of this motion which are, within experimental error, equal to those made available by CPMAS NMR for the tautomerism of the central hydrogens. In order to obtain further evidence for the presence of an overall molecular motion, the  $^{13}\text{C}$  CPMAS NMR spectra of porphine were recorded between 183 and 403 K. It was found that, in addition to the coalescence of the pyrrole carbon resonances due to the N-H tautomerism, the signals undergo a broadening process which can be explained in terms of a molecular motion. Again, the activation parameters which are obtained from these spectra are very similar to those measured for the central hydrogens migration. In view of these measurements, it is possible to revisit the significance of the X-ray structure of porphine as

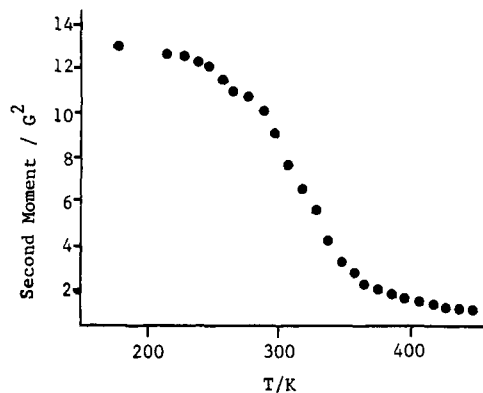


**Figure 2.** Second moment ( $M_2$ ) of the proton resonance line of porphine as a function of temperature.

well as to understand why the energies of the two tautomers of porphine are equal in the solid state.

### Experimental Section

Porphine was synthesized according to methods previously described in the literature<sup>24</sup> by heating 2-(hydroxymethyl)pyrrole in xylene at 110–115 °C in the presence of 0.7 M acetic acid. NMR spectra were recorded at 300 MHz on a VXR-300 NMR spectrometer and at 200 MHz on a home-built spectrometer and probe equipped with a B-VT100 temperature controller (temperatures are considered accurate within  $\pm 1$  °C). Good agreement between the data of the two equipments was found where measurements overlapped. In the home-built probe, precautions were taken to remove possible  $^1\text{H}$  stray signals which could otherwise spoil the experimental data.

$^{13}\text{C}$  CPMAS NMR spectra were recorded at 50.3 MHz on a home-built spectrometer equipped with a 7-mm Doty probe and at 25.16 MHz on an XL-100-15 spectrometer which was modified for performing the CP experiment and was equipped with a double-tuned home-built probe. The temperatures of the experiments carried out in this system were monitored by a thermocouple placed at the base of the spinner assembly and are considered accurate within  $\pm 2$  °C.

### Results

**$^1\text{H}$  NMR Analysis.** The second moments of the  $^1\text{H}$  signal of porphine measured at different temperatures are shown in Figure 2. The low-temperature values can be estimated from the available X-ray structure with Van Vleck's expression averaged over all orientations<sup>25</sup>

$$M_2^{\text{rigid}} = \frac{3}{5} \gamma_I^4 h^2 I(I+1) N_I^{-1} \sum_{i \neq j} r_{ij}^{-6} + \frac{4}{15} \gamma_I^2 \gamma_S^2 h^2 S(S+1) N_S^{-1} \sum_{i \neq j} r_{ij}^{-6} \quad (1)$$

where the first term is the contribution of the proton-proton dipolar interactions to the observed line width, the second term is the contribution of the proton-nitrogen dipolar interactions to the line width, and the sums run over all relevant nuclei. This expression and the available structure of porphine give an expected value of 30.5 kHz for the line width, close to the observed value of 34.5 kHz. The large decrease in the observed  $M_2$  may be ascribed to an in-plane rotation of the porphine macrocycle. The invariance of the dipolar Hamiltonian with respect to 180° rotations implies that the order of the rotation axis is greater than 2, and, although a diffusive rotational motion cannot be excluded, molecular symmetry considerations indicate that the most probable motion is a 90° flip about the main molecular axis. If this were the case, and assuming that intermolecular contributions to  $M_2$  are significantly suppressed by motion-induced modulation of  $\bar{r}_{ij}$ , the observed  $M_2$  when motion is faster than the spectral line width should be  $M_{2\text{total}}^{\text{motion}} \approx M_{2\text{intramolec}}^{\text{motion}} = 1/4 M_{2\text{intramolec}}^{\text{rigid}}$ .<sup>26</sup> Restricting

(15) Schlabach, M.; Wehrle, B.; Limbach, H.-H.; Bunnenberg, E.; Knierzinger, A.; Shu, A. Y. L.; Toff, B.-R.; Djerassi, C. *J. Am. Chem. Soc.* **1986**, *108*, 3856.

(16) Okazaki, M.; McDowell, C. A. *J. Am. Chem. Soc.* **1984**, *106*, 3185.

(17) Limbach, H.-H.; Hennig, J.; Kendrick, R.; Yannoni, C. S. *J. Am. Chem. Soc.* **1984**, *106*, 4059.

(18) Wehrle, B.; Limbach, H.-H.; Kocher, M.; Ermer, O.; Vogel, E. *Angew. Chem.* **1987**, *26*, 934.

(19) Frydman, L.; Olivieri, A. C.; Diaz, L. E.; Frydman, B.; Morin, F. G.; Mayne, C. L.; Grant, D. M.; Adler, A. D. *J. Am. Chem. Soc.* **1988**, *110*, 336.

(20) Frydman, L.; Olivieri, A. C.; Diaz, L. E.; Valasinas, A.; Frydman, B. *J. Am. Chem. Soc.* **1988**, *110*, 5651.

(21) (a) Chen, B. M. L.; Tulinsky, A. *J. Am. Chem. Soc.* **1972**, *94*, 4144.

(b) Tulinsky, A. *Ann. N. Y. Acad. Sci.* **1973**, *206*, pp 47 and ff. There is also an earlier analysis of the crystal structure of porphine (Webb, L. E.; Fleischer, E. B. *J. Chem. Phys.* **1965**, *43*, 3100), in which the central hydrogens were found delocalized over the four nitrogens. However, the crystal used in the latter study was contaminated with ca. 10% of the copper quelate, a fact that may have changed the crystal structure (see for example the discussion in ref 21b).

(22) Taylor, R.; Kennard, O. *Acc. Chem. Res.* **1984**, *17*, 320.

(23) Fyfe, C. A. *Solid State NMR for Chemists*; C. F. C. Press: Ontario, Canada, 1983; Chapter 2.

(24) Beytchman, S. D. Ph. D. Dissertation, University of Pennsylvania, 1966.

(25) (a) Van Vleck, J. H. *Phys. Rev.* **1948**, *74*, 1168. (b) Abragam, A. *The Principles of Nuclear Magnetism*; Oxford University Press: London, 1961; Chapters 4 and 9.

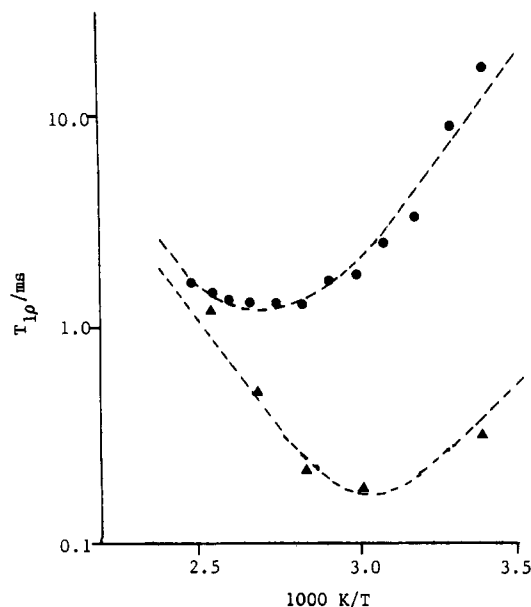


**Figure 3.** Temperature dependence of the  $^1\text{H}$  relaxation time  $T_{1\rho}$  for  $\gamma H_1 = 60$  kHz ( $\bullet$ ) and 40 kHz ( $\blacktriangle$ ). The dotted lines represent the best fit of eq 2 with correlation times defined as  $\tau(\bullet) = 2 \times 10^{-11} e^{4400/T}$ , and  $\tau(\blacktriangle) = 5 \times 10^{-12} e^{4900/T}$ .  $T_{1\rho}$  was measured using a  $90^\circ$  spin lock pulse sequence incorporating phase cycling, eight scans per spectrum, 60 s repetition time.

the sums in eq 1 to a single molecule, the X-ray predicts for an in-plane rotation a narrowing of the observed resonance to 13 kHz, in close agreement to the observed value (10.6 kHz).

Although an estimate of the activation energy involved in the process can be obtained from the onset temperature of the line narrowing by using Waugh's empirical equation  $E_a \approx 37 \cdot T$  cal  $\approx 37 \cdot 223$  cal = 8.25 kcal, the presence of molecular motions will manifest themselves in a large temperature dependence of the relaxation times, which can be interpreted quantitatively to determine activation energies. A convenient relaxation time for the analysis of motions which take place at a rate comparable to the observed line widths is the spin-lattice relaxation time in the rotating frame ( $T_{1\rho}$ ) that characterizes the decay of the magnetization along an on-resonance rf field  $H_1$

$$\frac{1}{T_{1\rho}} = C \left( \frac{5}{2} \frac{\tau_c}{1 + \omega_0^2 \tau_c^2} + \frac{\tau_c}{1 + 4\omega_0^2 \tau_c^2} + \frac{3}{2} \frac{\tau_c}{1 + 4\omega_1^2 \tau_c^2} \right) \quad (2)$$

where  $\omega_0 = \gamma H_0$ ,  $\omega_1 = \gamma H_1$ , and  $\tau_c$  is the correlation time of the process. Figure 3 shows a plot of  $\log T_{1\rho}$  against  $1/T$  for the magnetization of porphine at different  $\gamma H_1$  fields. A quantitative interpretation of this data is possible assuming that the correlation time obeys an Arrhenius-type temperature dependence  $\tau_c = \tau_0 e^{E_a/RT}$ . In the case under study, the correlation time of the process was found to have a preexponential factor  $\tau_0 = (1.25 \pm 0.75) \times 10^{-11}$  s and an activation energy  $E_a = (9.1 \pm 0.5)$  kcal/mol.

**$^{13}\text{C}$  CPMAS NMR Analysis.** One of the main drawbacks of a  $^1\text{H}$  wide line NMR study is, as its name may suggest, the lack of an appropriate spectral resolution. In consequence, unless one is dealing with simple molecules, it is usually difficult to discern which are the molecular mechanisms that originate the spectral changes that are observed. Porphine is not an exception to this rule. Although from the NMR point of view the molecule is not very complex, the fact that the molecules are already known to undergo a dynamic N-H tautomeric process may obscure the origin of the narrowing observed in the  $^1\text{H}$  NMR signal. Although Van Vleck's theory of moments appeared useful in order to evaluate the total line width of the signal at low temperatures and gave a good estimation for the expected line width in the case of a fast molecular rotation, there is no theoretical framework

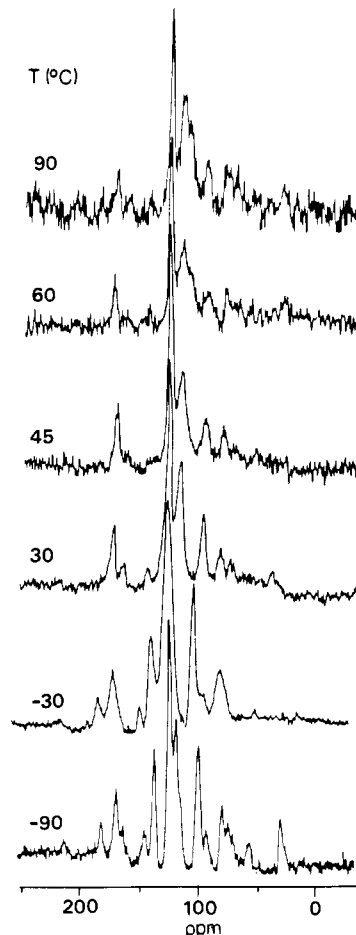


**Figure 4.** 50.3 MHz  $^{13}\text{C}$  CPMAS NMR spectra of porphine recorded at different temperatures. All the isotropic resonances fall between 99 and 149 ppm, and the smaller peaks appearing at multiples of 3.1 kHz from each centerband are spinning sidebands. 2000 scans with a 3 s repetition delay were acquired at each temperature. The low signal-to-noise ratio of the high-temperature spectra is probably due to the shortening of the  $^1\text{H}$   $T_{1\rho}$  described in Figure 3.

available in order to evaluate the separate contributions of the N-H tautomerism and of the overall molecular rotation to the decrease in the  $M_2$  that is shown in Figure 2. This fact, coupled to the similarity between the activation parameters available from Figure 3 and those measured previously for the central hydrogens migration process (see below), suggest the usefulness of an independent experiment in order to confirm the presence of molecular rotations.

In principle, there are two well-established mechanisms through which a molecular motion might affect a  $^{13}\text{C}$  CPMAS NMR spectrum: either by interfering with the coherent motion of the sample introduced by the magic-angle spinning process<sup>27</sup> or by interfering with the coherent motion of the spins introduced by the high-power proton decoupling.<sup>28</sup> Although both mechanisms can be thought to have a common origin, namely, that a stochastic motion tends to interfere with a coherent motion when both have similar rates, they possess different NMR time scales, and the maximum broadenings that they can introduce will be, in general, different. Interference with the MAS process will be relevant when the rates of the molecular motions are in the order of the chemical shift anisotropy (ca.  $10^3$  Hz), and the broadenings that they introduce will be larger as the magnetic field strength increases or the spinning speed of the sample decreases. On the other hand, high-power decoupling will be least efficient when the rates of

(27) (a) Suwelack, D.; Rothwell, W. P.; Waugh, J. S. *J. Chem. Phys.* **1980**, *73*, 2559. (b) Schmidt, A.; Vega, S. *J. Chem. Phys.* **1987**, *87*, 6895.

(28) (a) VanderHart, D. L.; Garrowsay, A. N. *J. Chem. Phys.* **1979**, *71*, 2773. (b) Rothwell, W. P.; Waugh, J. S. *J. Chem. Phys.* **1981**, *74*, 2721.

(26) Gutowsky, H. S.; Pake, G. E. *J. Chem. Phys.* **1950**, *18*, 162.

the motions are in the order of the Larmor frequency associated with the rf irradiation (ca.  $3 \times 10^4$  to  $10^5$  Hz), and the broadenings that will be observed will depend on the strength of the local field of the  $^{13}\text{C}$  nucleus under observation and on the decoupling power that is employed.

Figure 4 shows the 50.3 MHz  $^{13}\text{C}$  CPMAS NMR spectra of porphine recorded between  $-90^\circ\text{C}$  and  $90^\circ\text{C}$ . As could have been expected from previous reports,<sup>18,19</sup> the quenching of the N-H tautomerism at low temperatures originates the presence of two  $\alpha$ -carbon resonances at 149 and 133 ppm and of two  $\beta$ -carbon resonances at 133 and 124 ppm, in addition to the meso carbon signal appearing at 99 ppm (Figure 4,  $-90^\circ\text{C}$ ). As the temperature is increased, the activation of the N-H tautomerism induces the coalescence of the  $\beta$ -carbon signals (peak at 128 ppm in Figure 4,  $-30^\circ\text{C}$ ), which is followed by the coalescence of the  $\alpha$ -carbon signals (peak at 141 ppm in Figure 4,  $30^\circ\text{C}$ ). Although these are the only effects that can be expected due to the presence of the migration of the central hydrogens, the spectra show additional features as the temperature continues to increase. The most significant one is the broadening of the  $\beta$ - and the meso carbon resonances, which is already evident at  $30^\circ\text{C}$  and is maximum between  $60^\circ\text{C}$  and  $90^\circ\text{C}$ . Since it is not possible to explain this completely reversible effect by the presence of an N-H tautomerism, it is necessary to assume that the molecule is undergoing a second dynamic process, most likely an overall molecular rotation.

In order to analyze the broadenings that appear in the high-temperature spectra of porphine, it is convenient to evaluate the effects that will be introduced by the presence of  $90^\circ$  jumps of the molecules on the high-power decoupling and on the magic-angle spinning processes. For the case of the decoupling, it will be assumed that the dephasing introduced by the molecular motion in the  $^{13}\text{C}$  signal is given by<sup>28b</sup>

$$\frac{1}{T_2^{\text{DEC}}} = \frac{\gamma_{\text{H}}^2 \gamma_{\text{C}}^2 \hbar^2}{5 r_{\text{CH}}^6} \frac{\tau_{\text{c}}}{1 + \omega_1^2 \tau_{\text{c}}^2} \quad (3)$$

where  $\tau_{\text{c}}$ ,  $\omega_1$  are as in eq 2, and  $r_{\text{CH}}$  is the distance between the nucleus under consideration and its nearest proton. Although this simple equation has been derived for the ideal case of isotropic molecular motions, negligible  $^1\text{H}$ - $^1\text{H}$  dipolar interactions, and for  $^{13}\text{C}$  nuclei coupled to only one  $^1\text{H}$ , its predictions have been shown to closely follow the behavior of more real systems.<sup>28b</sup> On the other hand, the influence of  $90^\circ$  jumps on the MAS process can be evaluated by solving for each nuclei the set of differential equations

$$\begin{aligned} \frac{d}{dt} M_{\text{A}}(\alpha, \beta, \gamma; t) &= i\omega_{\text{A}}(\alpha, \beta, \gamma; t) M_{\text{A}}(t) + \frac{M_{\text{B}}(t) - M_{\text{A}}(t)}{\tau_{\text{c}}} \\ \frac{d}{dt} M_{\text{B}}(\alpha, \beta, \gamma; t) &= i\omega_{\text{B}}(\alpha, \beta, \gamma; t) M_{\text{B}}(t) + \frac{M_{\text{A}}(t) - M_{\text{B}}(t)}{\tau_{\text{c}}} \end{aligned} \quad (4)$$

where  $\alpha$ ,  $\beta$ , and  $\gamma$  are the Euler angles that relate a reference frame fixed on the molecule with a reference frame fixed on the rotor;  $\omega_{\text{A}}$  and  $\omega_{\text{B}}$  are the resonance frequencies of the two sites which are related by a  $90^\circ$  rotation around the main molecular axis; and the invariance of the chemical shift tensor with respect to  $180^\circ$  rotations has been used in order to reduce the problem from a four-site to a two-site exchange process. The time dependence introduced in  $\omega_{\text{A}}$  and  $\omega_{\text{B}}$  by the sample spinning precludes an analytical solution of eq 4 which was therefore solved numerically by replacing the two time-dependent frequencies by three pairs of time-independent frequencies.<sup>29</sup> The final spectrum for a given rate  $\tau_{\text{c}}$  can be obtained by integration of  $M_{\text{A}}$ ,  $M_{\text{B}}$  over all the possible  $0^\circ \leq \alpha, \beta, \gamma \leq 180^\circ$  orientations, followed by an exponential weighting and a Fourier transformation of  $M_{\text{A}}(t) + M_{\text{B}}(t)$ . Although the simulations that are described in the present study could have focused on the  $\alpha$ -, the  $\beta$ -, or the meso carbon resonances, signal-to-noise considerations made an analysis of the latter signal uncertain. In order to evaluate the effects of the motion on the signals of the other carbons it is necessary to estimate a

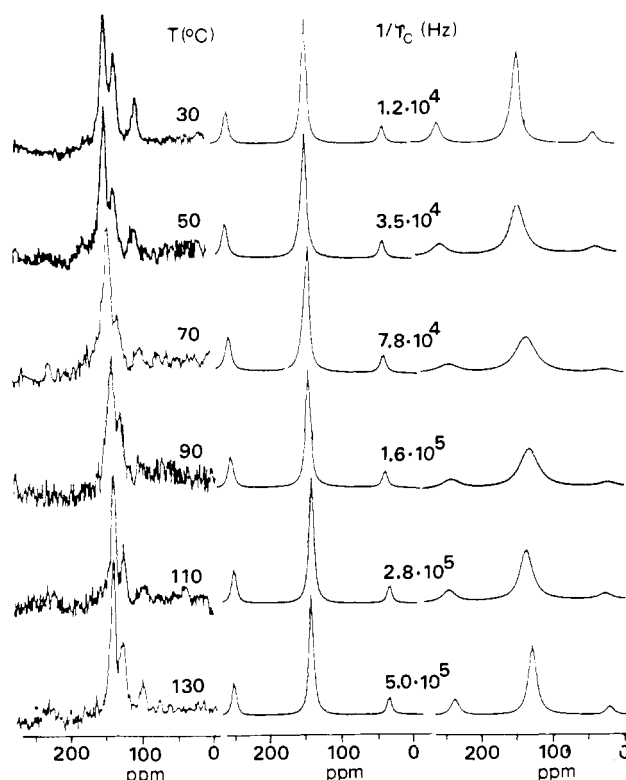


**Figure 5.** Experimental (left-hand column) and simulated line shapes of the  $^{13}\text{C}$  CPMAS NMR spectra of porphine at 25.16 MHz. An average of 55 000 transients were acquired at each temperature. Other special parameters are 3 s pulse delay, 1.5 ms contact time, 8 Hz line broadening, 70 kHz decoupling field, and 2.6 kHz spinning speed. For the  $\alpha$ -carbon simulations (center column) a nonexchanging line width of 150 Hz was used, a value which probably includes the effects of the residual dipolar coupling between the  $^{13}\text{C}$  and the  $^{14}\text{N}$ . For the  $\beta$ -carbon simulations (right-hand column) a nonexchanging line width of 30 Hz was used. Since the same scaling factor was used in all the simulations, the differences in the heights of the peaks reflect the effects of the line broadenings. The fact that the spinning sidebands of the experimental spectra are lost in the base line noise is probably due to instabilities in the rates of rotation during the long accumulation times (ca. 48 h) that were used for each spectra.

value for the  $r_{\text{CH}}$  to be used in eq 3 as well as the approximate values of the chemical shielding tensor at each site to be used in eq 4. For the  $\beta$ -carbons it was assumed that  $r_{\text{C}\beta\text{-H}} = 1.15 \text{ \AA}$  and that the chemical shift parameters of these carbons are similar to those of benzene ( $\omega_{xx} = 235$ ,  $\omega_{yy} = 145$ ,  $\omega_{zz} = 10$  ppm). For the  $\alpha$ -carbons two dipolar interactions were assumed, each one characterized by a distance  $r_{\text{C}\alpha\text{-H}} = 2.15 \text{ \AA}$ . The chemical shift parameters of these carbons were taken as  $\omega_{xx} = 212$ ,  $\omega_{yy} = 184$ ,  $\omega_{zz} = -8$  ppm on the basis of the similarity in the chemical environments between the  $\alpha$ -carbons and the external bridgehead carbons of pyrene.<sup>30</sup>

The left-hand column of Figure 5 shows the 25.16 MHz  $^{13}\text{C}$  CPMAS NMR spectra of porphine recorded at different temperatures. In order to get the correlation time of the motion at each temperature, a pool of the time-domain signals arising from eq 4 was computed for different values of  $\tau_{\text{c}}$ , multiplied by

$$e^{-t(1/T_2^0 + 1/T_2^{\text{DEC}})}$$

(where  $1/T_2^0$  takes into account the nonexchanging line width), Fourier transformed and compared with the different experimental spectra. The results of these simulations are shown in the center ( $\alpha$ -carbons) and in the right-hand ( $\beta$ -carbons) columns of Figure 5, together with the rates used for each temperature. From these simulations it could be concluded that although motional modulation of the MAS process is the main factor in the broadenings

(29) Frydman, L.; Frydman, B., submitted for publication.

(30) Carter, C. L.; Alderman, D. W.; Facelli, J. C.; Grant, D. M. *J. Am. Chem. Soc.* **1987**, *109*, 2639.

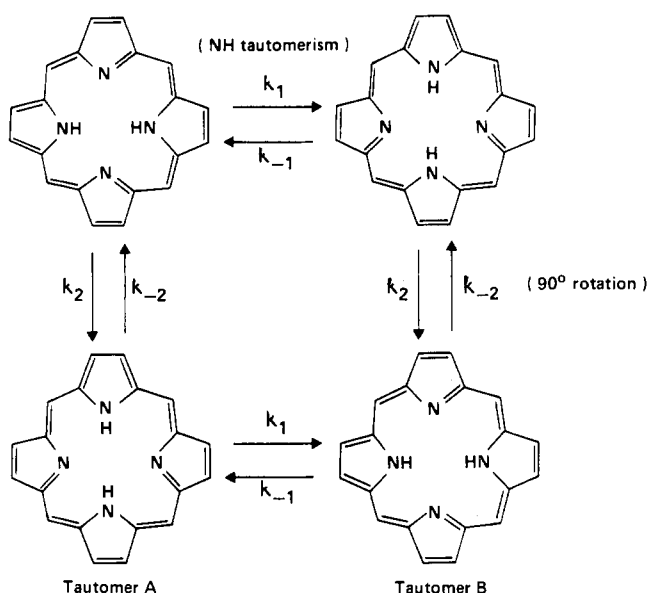


**Figure 6.** Possible rearrangements in solid porphine. The X-ray analysis of porphine detects only one hydrogen configuration (e.g., the one shown on the upper left and on the lower right). CPMAS NMR measures at room temperature a tautomerization process (1) with  $k_1 = k_{-1}$  that is fast on the NMR time scale. It is possible to reconcile X-ray and CPMAS NMR data assuming that there is a second process (2) determined by  $k_2$  and  $k_{-2}$  that involves a  $90^\circ$  rotation of the molecules in the crystal: the passage from the configurations of the upper row to those of the lower row involves no bond breaking.

observed below  $50^\circ\text{C}$ , inefficient decoupling produces the significant broadenings which are observed at higher temperatures. From the rate constants used in the simulations at each temperature, an Arrhenius equation can be obtained for the correlation time of the process which is very similar to the one obtained from the  $^1\text{H}$  relaxation data ( $\tau_0 = (3.0 \pm 1.5) \times 10^{-11}\text{ s}$ ,  $E_a = (9.0 \pm 0.8)\text{ kcal/mol}$ ). Therefore, the analysis of the  $^{13}\text{C}$  NMR results is not only able to give an estimation of the activation parameters but is also useful to validate the interpretation given to the  $^1\text{H}$  NMR data.

### Discussion

The fact that the porphine molecules rotate in the solid is not able by itself to resolve the contradiction between the localized hydrogens detected by X-ray and the solution-like tautomerism revealed by CPMAS NMR. On the contrary, although the rotation of the molecules can explain the fact that the energies of the two tautomers in the crystal are equal, a new problem is introduced, namely, why if the molecules in the solid are rotating

they appear distorted toward a  $D_{2h}$  symmetry in the X-ray diffraction analysis. This seeming contradiction can be explained if it is assumed that the migration of the central hydrogens is coupled to a  $90^\circ$  rotation of the molecules about their main axes (Figure 6). In this way, neither the hydrogens migration nor the macrocycles rotation would disturb the translational symmetry of the crystal. Recently,<sup>18</sup> a line shape analysis of the CPMAS NMR spectra of porphine allowed for the measure of the correlation times of the N-H tautomerization process at different temperatures, which were found to follow an Arrhenius-type dependence  $\tau_{\text{taut}} = 10^{-11}e^{4774/T}$ . Since the activation parameters which characterize the motion of the macrocycle are equal, within experimental error, to those which can be found for the motion of the central hydrogens, the proton localization observed by X-ray favors the presence of the combined motion mentioned above. It should be noted that this conclusion could not have been reached with only the X-ray, the CPMAS NMR, or the  $^1\text{H}$  wide line NMR results; it is a picture which only emerges when the three experiments are considered together.

If both dynamical processes would be coupled, the deformation of the porphine skeleton which is shown by X-ray would suggest that there is a skeletal rearrangement coupled to the hydrogens migration, a fact that if further confirmed could contribute to the understanding of the mechanism of the tautomerization process. The motion found for the porphine molecules, which is very likely responsible for the symmetry of the double minimum potential of the hydrogen transfer, is probably absent in a bulky molecule like tetratolylporphyrin although in the latter the hydrogen migration is not affected on the average by crystal packing forces.<sup>17</sup> Nevertheless, it cannot be discarded that such a motion is present in a planar molecule like phthalocyanine which shows in the solid a fast hydrogen tautomerism,<sup>31</sup> a possibility which is actually under evaluation. It could also be of interest to measure the effects of replacing the central hydrogens of porphine by deuteriums, since if the skeletal motion would be coupled to the tautomerization process it should be affected (in an indirect manner) by the kinetic isotope effect of the tautomerism.

**Acknowledgment.** This research was supported in part by the National Institutes of Health under Grant GM 11973 and by the Consejo Nacional de Investigaciones Científicas y Técnicas (CONICET). A.C.O. and L.F. are grateful to CONICET for Fellowships. Support from the Fundacion Campomar-Weizmann Institute of Sciences exchange program is also gratefully acknowledged.

**Registry No.** Porphine, 101-60-0.

(31) (a) Kendrick, R. D.; Friedrich, S.; Wehrle, B.; Limbach, H. H.; Yannoni, C. S. *J. Magn. Reson.* **1985**, *65*, 159. (b) Meier, B. H.; Storm, C. B.; Earl, W. L. *J. Am. Chem. Soc.* **1986**, *108*, 6072.